



¹. M. S. DADA

RADIATION, DISSIPATION AND MHD EFFECTS ON FLUID FLOW PAST AN IMPULSIVELY STARTED VERTICAL NEWTONIAN HEATING PLATE

¹. DEPARTMENT OF MATHEMATICS, UNIVERSITY OF ILORIN, ILORIN, NIGERIA

ABSTRACT: The combined effects of dissipation, thermal radiation and MHD on the viscous incompressible unsteady fluid flow past an impulsively started infinite vertical plate with Newtonian heating for optically thin radiation limit case is investigated. The set of governing boundary layer equations is transformed to its non-dimensional forms and solved for the temperature and velocity distributions by Crank Nicolson implicit finite difference method. The effects of radiation parameter, magnetic field parameter, Grashof number, Eckert number and Prandtl number on the velocity and temperature profiles, and on the skin friction are illustrated in graphical and tabular forms. The contributions of the various material parameters on the flow field are highlighted.

KEYWORDS: Viscous dissipation, Thermal radiation, MHD, Newtonian heating

INTRODUCTION

The modeling of radiative magneto hydrodynamic fluid flow is significant from geophysics, engineering and astrophysics points of view. It has several physical applications such as in some matters at high temperature, some engineering devices can be ionized and become an electrical conductor. The ionized matters (gas or plasma) can be made to interact with the magnetic field and alter heat transferred and friction characteristics [6]. As the case in this study, the unsteady boundary layer problems have many real applications in flows over blades of compressors and turbines, over aerodynamic surfaces of vehicles in manned flight and over a helicopter in translation motion. Also, the conjugate convective flow known as Newtonian heating, where heat transfer rate from the boundary surface is proportional to the local surface temperature occurs in many important engineering devices and it has been noted that the convective assumption of no interaction of conduction coupled effects is not always realistic [2].

Several studies have been reported on an impulsively started vertical plate with some boundary conditions. Earlier, Stewarton [9] and Soundalgekar [10] presented analytical solutions on the impulsive motion of a flat plate in a viscous fluid and free convection effects on the Stoke problem for infinite vertical plate respectively.

The above studies considered the fluid as electrically non-conducting. On the contrary, the influence of magnetic field on electrically conducting fluid is of great importance in high speed aerodynamics astronautically plasma flows MHD boundary layer control, MHD accelerator technologies etc [8]. To this effect, Soundalgekar et al [11] presented a study on free convection effects on the MHD Stoke problem for a vertical plate.

The effects of thermal radiation on fluid flow have led some researchers to carry out studies on the influence of thermal radiation on the fluid flows. Notable among them are Takhar H.S. et al [12] who reported on the radiation effects on MHD free convection flow of a radiating fluid past a semi-infinite vertical plate. Abd El-Naby, M. A. et al [1] studied the finite difference solution of radiation effects on MHD unsteady free convection flow over a vertical plate with variable surface temperature. The effects of the interaction of both MHD and thermal radiation was reported by Mazumdar, M.K. and Dekar, R. K. [6] in their investigation titled MHD flow past an impulsively started infinite vertical plate in presence of thermal radiation.

In the above investigations, viscous dissipation term is neglected. The exclusion of viscous dissipation function removes the non-linear dissipation term from the governing equation and hence it presented a simplified version of the equation. The important effects of dissipation in geophysical flow and in higher operating temperature led Isreal-Cookey et al [4] to investigate the influence of viscous dissipation on unsteady MHD free convection flow past and infinite vertical plate in porous medium with time-dependent suction. Also, Zucco Jordan, J [13] studied Network simulation method applied to radiation and dissipation effects on MHD unsteady free convection over vertical porous plate.

In all the studies mentioned above, the flow is characterized by a prescribed surface temperature or a surface heat flux. Recently, Newtonian heating surface condition has attracted the interest of some

researchers because of its important applications in engineering devices [2]. Initial study on the newtonian heating surface was carried out by Merkin, J. H. [7] who studied natural convection boundary layer flow on a vertical surface with Newtonian heating. Recently, Lesnic D et al [5] carried out their investigations on the steady free convection boundary layer flow with Newtonian heating surface in porous media.

On this note, unsteady free convection boundary layer flow past an impulsively started vertical surface with Newtonian heating was carried out using Laplace transform technique by R.C.Chaudhary, Preeti Jain [2]. The above study on unsteady free convection boundary layer flow past a vertical surface with Newtonian heating neglected radiative, dissipative and magnetic field parameters.

Hence, this paper investigates the effects of radiation, dissipation and magnetic field on the viscous incompressible fluid flow past an impulsively started vertical plate with Newtonian heating for an optically thin limit case.

MATHEMATICAL FORMULATION

Consider the unsteady free convective flow of a radiating viscous incompressible and electrical conducting fluid past an impulsively started infinite vertical plate with Newtonian heating. The \hat{x} -axis is taken along the plate in the vertical upward direction and the \hat{y} -axis is normal to the plate in the direction of the applied magnetic field. Initially, the plate and the fluid assumed the same temperature T_∞ at the time $t \leq 0$. At time $t > 0$, the plate is given an impulsive motion in the vertical upward direction against gravitational field with a velocity U_0 . The rate of heat transfer from the surface is assumed to vary directly to the local surface temperature T . As the plate is considered infinite in \hat{x} -direction, all the physical variables are function of \hat{y} and t only. Then, the fully developed flow of a radiating gas is governed by the following set of equations under the usual Boussinesq's approximation:

$$\frac{\partial \hat{U}'}{\partial \hat{t}} = \nu \frac{\partial^2 \hat{U}'}{\partial \hat{y}^2} + g\beta (\hat{T} - \hat{T}_\infty) - \frac{\sigma \beta_0^2 \hat{U}}{\rho} \quad (1)$$

$$\rho c_p \frac{\partial \hat{T}'}{\partial \hat{t}} = k \frac{\partial^2 \hat{T}'}{\partial \hat{y}^2} + \mu \left(\frac{\partial \hat{U}'}{\partial \hat{y}} \right)^2 - \frac{\partial q_r}{\partial \hat{y}} \quad (2)$$

with the following initial and boundary conditions

$$\begin{aligned} \hat{t} \leq 0, \quad \hat{U} &= 0, \quad \hat{T} = \hat{T}_\infty \quad \text{for all } \hat{y} \\ \hat{t} > 0, \quad \hat{U} &= \hat{U}_0, \quad \frac{\partial \hat{T}}{\partial \hat{y}} = -\frac{h\hat{T}}{\kappa} \quad \text{at } \hat{y} = 0 \\ \hat{U} &\rightarrow 0, \quad \hat{T} \rightarrow \hat{T}_\infty \quad \text{as } \hat{y} \rightarrow \infty. \end{aligned} \quad (3)$$

where \hat{U} is a velocity component in \hat{x} -directions, ρ is the density, g is the acceleration due to gravity, \hat{T} is the temperature of the fluid, c_p is the specific heat at constant pressure, β is the coefficient of thermal expansion, κ is the thermal conductivity, q_r is the radiative flux and σ is the electrical conductivity. ν is the kinematic viscosity, μ is the viscosity of the fluid, h is the heat transfer coefficient and B_0 is the strength of the magnetic field. The equation of continuity is identically satisfied.

In the optically thin limit, the fluid does not absorb its own emitted radiation which implies that there is no self-absorption but rather the fluid absorbs radiation emitted by the boundaries. For non-grey gas near equilibrium in the optically thin limit case, Cogly, Vincentine and Gillies [3] showed that

$$\frac{\partial q_r}{\partial \hat{y}} = 4(\hat{T} - \hat{T}_\infty) \quad (4)$$

where $I = \int_0^\infty \kappa_{\lambda_w} \left(\frac{de_{b\lambda}}{d\hat{T}} \right) d\lambda$, κ_{λ_w} is the absorption coefficient, $e_{b\lambda}$ is the planck function and the subscript

w indicates the values at the wall.

Introducing the following dimensionless quantities

$$U = \frac{\hat{U}}{\hat{U}_0}, \quad t = \frac{\hat{t} \hat{U}_0^2}{\nu}, \quad y = \frac{\hat{y} \hat{U}_0}{\nu} \quad (5)$$

equations (1) and (2) respectively become

$$\frac{\partial U}{\partial i} = \frac{\partial^2 U}{\partial y^2} + G\theta - MU \tag{6}$$

$$\frac{\partial \theta}{\partial i} = \frac{1}{Pr} \frac{\partial^2 \theta}{\partial y^2} + Ec \left(\frac{\partial U}{\partial y} \right)^2 \tag{7}$$

where $Pr = \frac{c_p \mu}{\kappa}$ is the Prandtl number, $F = \frac{4I\nu}{\rho \alpha_p U_0^2}$ is the radiation parameter, $M = \frac{\nu \alpha B_0^2}{\rho U_0^2}$ is the magnetic

field parameter, $Ec = \frac{U_0^2}{c_p T_\infty}$ is the Eckert number, $G = \frac{\nu g \beta T_\infty}{U_0^3}$ is the Grashof number and $\theta = \frac{T - T_\infty}{T_\infty}$.

The initial and boundary conditions (3) in dimensionless forms become

$$\begin{aligned} t \leq 0, \quad U = 0, \quad \theta = 0 \quad \text{for all } y \\ t > 0, \quad U = 1, \quad \frac{\partial \theta}{\partial y} = (\theta + 1) \quad \text{at } y = 0 \\ U \rightarrow 0, \quad \theta \rightarrow 0 \quad \text{as } y \rightarrow \infty. \end{aligned} \tag{8}$$

where velocity U_0 takes the form $U_0 = \frac{h\nu}{\kappa}$

From the velocity field, the skin friction is given by

$$\tau = \mu \left. \frac{\partial U}{\partial y} \right|_{y=0}$$

which, in view of equation (5), is expressed in dimensionless form as

$$\tau = \left. \frac{\partial U}{\partial y} \right|_{y=0} \tag{9}$$

NUMERICAL TECHNIQUE AND DISCUSSION

To solve the unsteady non-linear coupled partial differential equations (6) and (7) under the initial and boundary conditions (8), an implicit finite difference method of Crank Nicolson type is used. This method converges fast and unconditionally stable [8].

The finite difference equations corresponding to equations (7) and (8) are discretized using Nicolson method as follows:

$$\frac{U_i^{n+1} - U_i^n}{\Delta t} = \frac{U_{i-1}^{n+1} - 2U_i^{n+1} + U_{i+1}^{n+1} + U_{i-1}^n - 2U_i^n + U_{i+1}^n}{2(\Delta y)^2} + G \left(\frac{\theta_i^{n+1} + \theta_i^n}{2} \right) + M \left(\frac{U_i^{n+1} + U_i^n}{2} \right) \tag{10}$$

$$\frac{\theta_i^{n+1} - \theta_i^n}{\Delta t} = \frac{\theta_{i-1}^{n+1} - 2\theta_i^{n+1} + \theta_{i+1}^{n+1} + \theta_{i-1}^n - 2\theta_i^n + \theta_{i+1}^n}{2Pr(\Delta y)^2} + Ec \left(\frac{U_{i-1}^n - U_i^n}{2\Delta y} \right)^2 + F \left(\frac{\theta_i^{n+1} + \theta_i^n}{2} \right) \tag{11}$$

The initial and boundary conditions may be expressed as

$$\begin{aligned} U_i^0 = 0, \quad \theta_i^0 = 0 \quad \text{for all } i \text{ except for } i = 0 \\ U_0^{n+1} = 1, \quad \theta_0^{n+1} = \theta_2^{n+1} + 2\Delta y \theta_1^{n+1} + 2\Delta y \quad \text{for } i = 0, \quad U_{\max}^{n+1} = 0 \end{aligned} \tag{12}$$

Also, $U_0^n = 1, \quad \theta_0^n = \theta_2^n + 2\Delta y \theta_1^n + 2\Delta y$ for $i = 0, \quad U_{\max}^n = 0$

where max corresponds to ∞ . Equations (10) and (11) may be written as follows:

$$\begin{aligned} -rU_{i-1}^{n+1} + (1+2r+k_1)U_i^{n+1} - rU_{i+1}^{n+1} \\ = rU_{i-1}^n + (1-2r-k_1)U_i^n - rU_{i+1}^n - s \end{aligned} \tag{13}$$

$$\begin{aligned} -R\theta_{i-1}^{n+1} + (1+2R+F_1)\theta_i^{n+1} - R\theta_{i+1}^{n+1} \\ = R\theta_{i-1}^n + (1-2R-F_1)\theta_i^n - R\theta_{i+1}^n + P(U_{i+1}^n - U_{i-1}^n)^2 \end{aligned} \tag{14}$$

where $r = \frac{\Delta t}{2(\Delta y)^2}$, $k_1 = \frac{M\Delta t}{2}$, $s = \frac{G\Delta t}{2}$, $F_1 = \frac{F\Delta t}{2}$, $P = \frac{rEc}{2}$, $R = \frac{r}{Pr}$.

The subscript $i = \max$ is far outside the thermal and momentum boundary layers. The maximum of y was arrived at after the initial investigations to ensure that the last two boundary conditions (8) are satisfied. Here the subscript i and superscript n denote the grid points along the y - and t -directions

respectively. The values of U and ϑ . are known at all grid points at $t=0$ from the initial conditions. The computation of U and ϑ . at the $(n+1)$ th time using the values at previous (n) th time are carried out as follows:

Having known, at all grid points, the values of ϑ . and U at time $t_1=0$ from the initial conditions, the values of ϑ . at time $t_2=t_1+\Delta t$. are calculated using the known values at previous time $t = t_1$, as follows: The finite difference equation (14) forms a tri-diagonal system of equations where the values of ϑ . at every nodal point at time $t_2=t_1+\Delta t$. are determined using the known values at previous time $t = t_1$. This tri-diagonal system of equations is solved using Thomas algorithm. Hence, the values of ϑ . at every nodal point at time $t_1+\Delta t$. are known. The known values of ϑ . at time $t_1+\Delta t$. and values of U and θ . at previous time $t = t_1$ are used in equation (13). Similarly, the values of U are computed at time $t_2 = t_1 + \Delta t$. This procedure is followed until the values of U and ϑ . are obtained for the required time.

The computation are carried out for different values of Prandtl number Pr , Eckert number Ec , Magnetic field parameter M , Radiation parameter F and Grashof number G in order to study the influences of these parameters on the fluid flow.

The velocity distribution profiles with variation of Eckert number Ec and Grashof number G are shown in Figures 1 and 2 respectively. Other parameters are kept constant. It is observed that an increase in Eckert number causes the velocity to increase. Similarly, when the Grashof number is increased, the velocity of the fluid also increases. The viscous dissipation heat parameter which is often neglected causes a rise in velocity of the fluid. The velocity near the wall rises rapidly and descends gradually to zero as its distance from the plate increases.

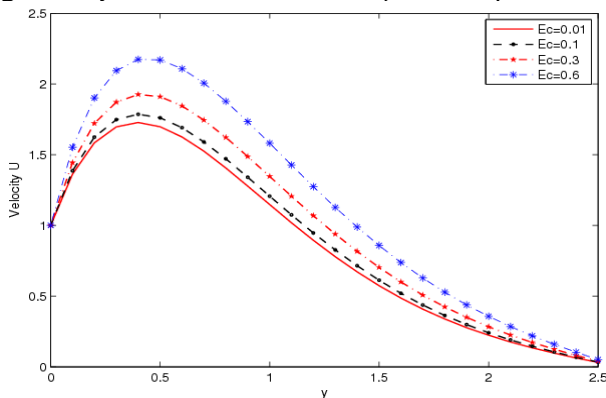


Figure 1. The velocity distribution profiles with variation of Eckert number Ec at time $t=0.6$ and for fixed parameters $Pr=0.71$, $F=1$, $G=8$ and $M=1$

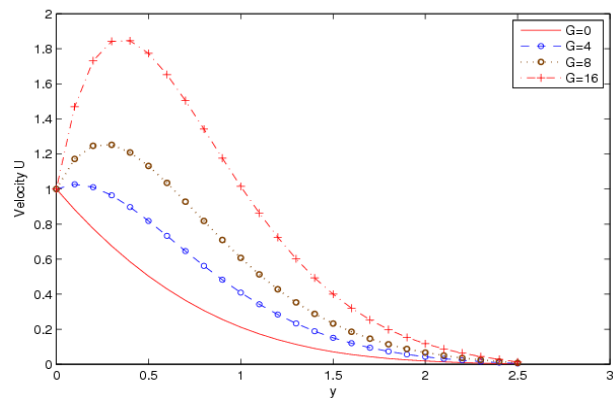


Figure 2. The velocity distribution profiles with variation of Grashof number G at time $t=0.4$ and for fixed parameters $Pr=0.71$, $F=1$, $Ec=0.1$ and $M=1$.

Figures 3 and 4 illustrate the thermal distribution profiles with variation of Eckert number Ec and Grashof number G . A rapid drop in temperature is noticed in the fluid as one moves farther from the plate. The viscous heat dissipative parameter Ec accelerates the temperature. Moreover, increasing Grashof G number causes a rise in the temperature of the fluid.

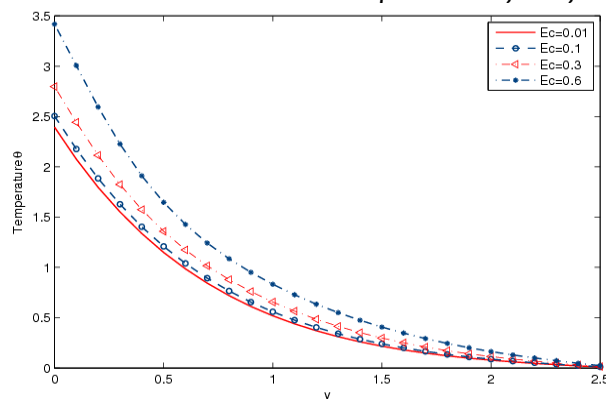


Figure 3. The thermal distribution profiles with variation of Eckert number Ec at time $t=0.6$ and for fixed parameters $Pr=0.71$, $F=1$, $G=8$ and $M=1$

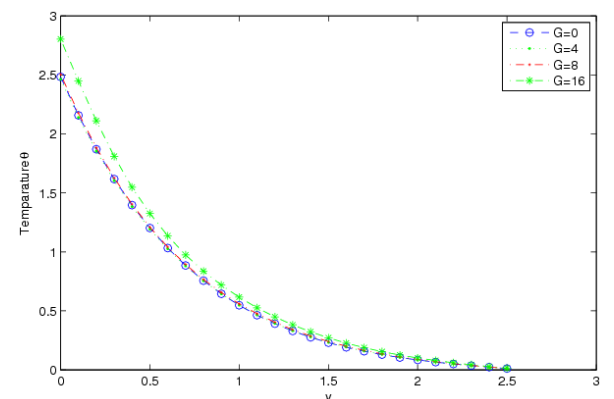


Figure 4. The thermal distribution profiles with variation of Grashof number G at time $t=0.4$ and for fixed parameters $Pr=0.71$, $F=1$, $Ec=0.1$ and $M=1$

In Figures 5, 6 and 7, the velocity distribution profiles for variation of radiation parameter F , magnetic fluid parameter M and Prandtl number Pr respectively are shown with all other parameters kept constant, it can be seen that the velocity is reduced by increasing the value of magnetic field parameter M , Radiation parameter F or Prandtl number Pr .

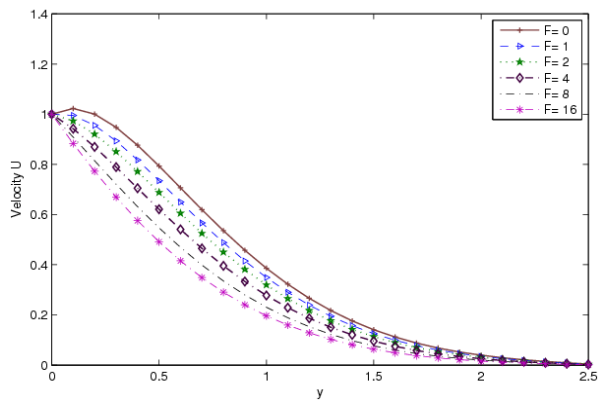


Figure 5. The velocity distribution profiles with variation of radiation parameter F at time $t=0.4$ and for fixed parameters $G=4$, $Pr=0.71$, $Ec=0.1$ and $M=2$

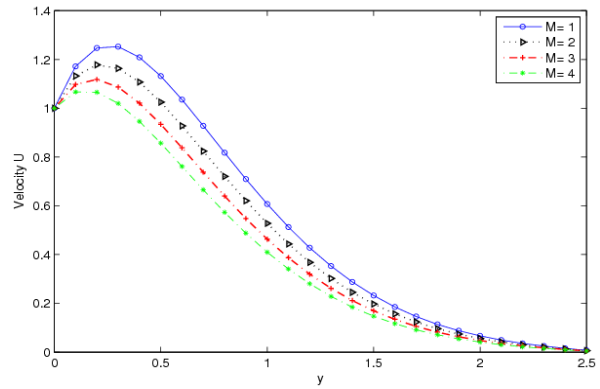


Figure 6. The velocity distribution profiles with variation of magnetic field parameter M at time $t=0.4$ and for fixed parameters $Pr=0.71$, $F=1$, $Ec=0.1$ and $G=8$

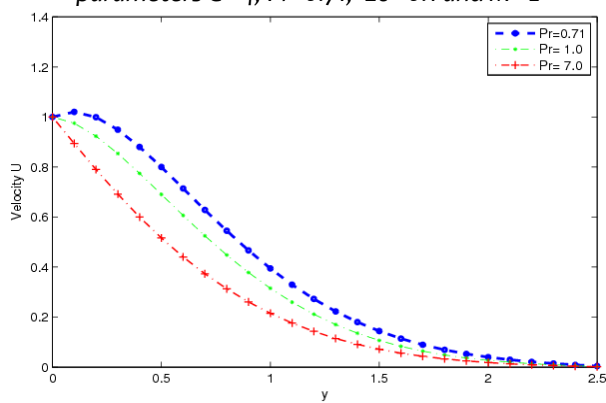


Figure 7. The velocity distribution profiles with variation of Prandtl number Pr at time $t=0.4$ and for fixed parameters $G=4$, $F=1$, $Ec=0.01$ and $M=1$

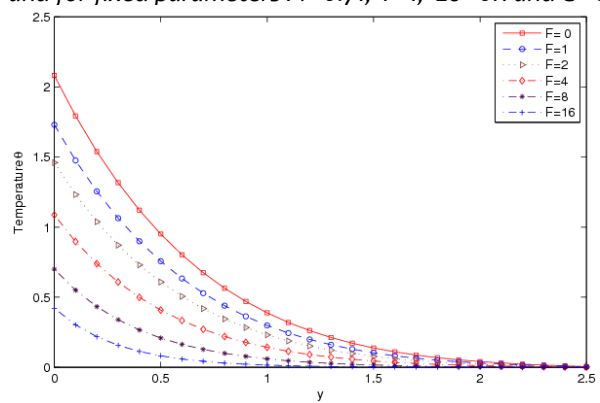


Figure 8. The thermal distribution profiles with variation of radiation parameter F at time $t=0.4$ and for fixed parameters $G=4$, $Pr=0.71$, $Ec=0.1$ and $M=2$

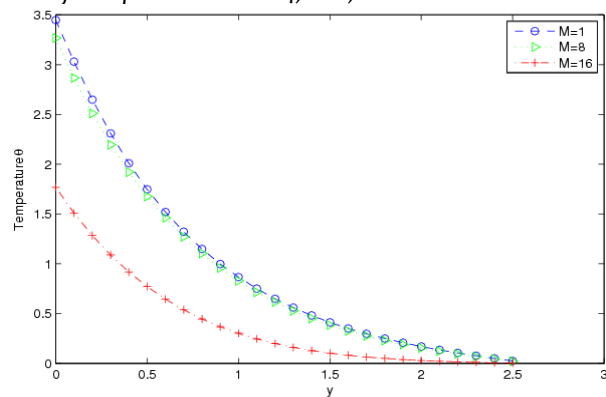


Figure 9. The thermal distribution profiles with variation of magnetic field parameter M at time $t=0.8$ and for fixed parameters $Pr=0.71$, $F=1$, $Ec=0.1$ and $G=8$

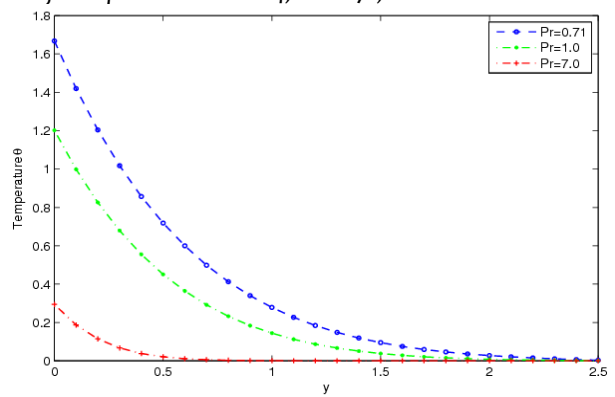


Figure 10. The thermal distribution profiles with variation of Prandtl number Pr at time $t=0.4$ and for fixed parameters $G=4$, $F=1$, $Ec=0.01$ and $M=1$

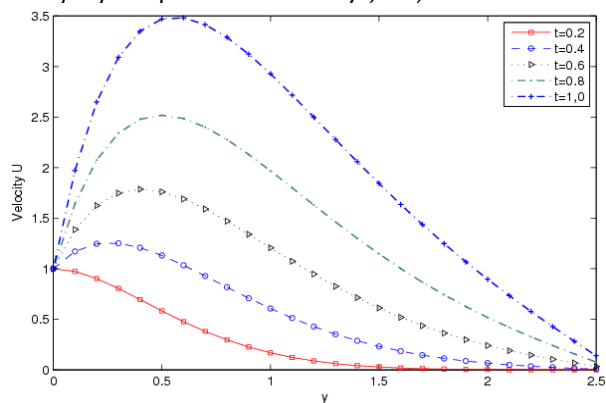


Figure 11. The velocity distribution profiles with variation of time for fixed parameters $Pr=0.71$, $F=1$, $Ec=0.1$ and $G=8$

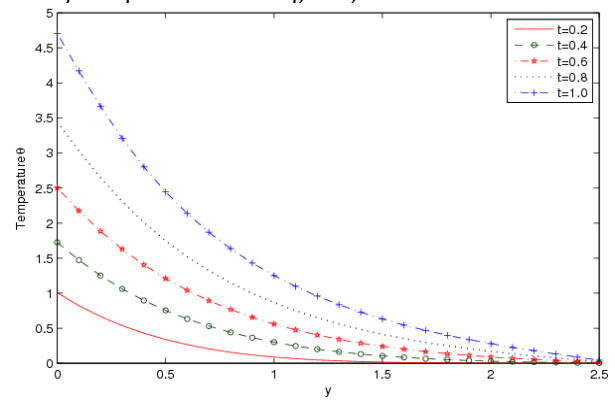


Figure 12. The thermal distribution profiles with variation of time for fixed parameters $Pr=0.71$, $F=1$, $Ec=0.1$ and $G=8$

Figures 8, 9 and 10 illustrate the thermal distribution profiles with the variation of radiation parameter F , magnetic fluid parameter M and Prandtl number Pr respectively. It is observed that increasing each of the radiation parameter F , magnetic field parameter M and Prandtl number Pr produces significant decrease in the thermal condition of the fluid.

The variation of time with velocity and thermal profiles, as shown in Figures 11 and 12, reveals that temperature and velocity increase as the time increases.

The skin friction τ is shown in Table 1 for various values of radiation parameter F , magnetic field parameter M , Grashof number G , Eckert number Ec and Prandtl number Pr . In order to highlight the contributions of each parameter, one parameter is varied while the rest others take default fixed values which are $F=1$, $Pr=1.0$, $G=2$, $M=2$ and $Ec=0.3$. It is observed that an increase in skin friction results in an increase in each of the parameters Pr , M and F . But, the wall shear stress as evidence in this table decreases as the Grashof number Gr and Eckert number Ec increases. That is, increasing Grashof number serves to decrease the shearing stress on the wall and increasing viscous dissipative heat serves to reduce the shearing stress on the surface.

Also, the wall shear stress decreases as the value of the time t increases for a constant value of radiation parameter F , magnetic field parameter M , Grashof number G , Eckert number Ec or Prandtl number Pr .

CONCLUSIONS

A mathematical model has been presented for the unsteady dissipative MHD convective flow past an impulsively started plane with Newtonian heating in the presence of thermal radiation. The governing boundary layer equations have been transformed into non-dimensional forms and solved using the implicit finite difference method of Crank Nicolson type. It has been shown that velocity and temperature increase with an increase in Grashof number G or Eckert number Ec . Also, the temperature and velocity increase with time t . An increase in Prandtl number, radiation parameter or magnetic field parameter lowers the velocity and temperature.

Furthermore, there is a rise in the skin friction due to greater Prandtl number, magnetic field parameter or radiation parameter while a fall is observed in skin friction with increase in Grashof number or Eckert number.

REFERENCES

- [1.] Abd El-Naby, M. E.; Elbarbary, E. M. E. and Abdelazem, N. Y.: Finite difference solution of radiation effects on MHD unsteady free-convection flow over vertical plate with variable surface temperature, *J. Appl. Math.*, (2), 65-86, 2003.
- [2.] Chaudhary, R. C. and Jain, P.: Unsteady free convection boundary layer flow past an impulsively started vertical surface with Newtonian heating, *Romanian Journal of Physics*, (51) 9, : 911 - 925, 2007.
- [3.] Cogly, A. C.; Vincentine, W. C. and Gilles, S. E.: Differential approximation for radiative transfer in a non-gray near equilibrium, *AIAA Journal*, {6}, 551-555, 1968.
- [4.] Isreal-Cookey, C.; Ogulu, A. and Omubo-Pepple, V. M. : Influence of viscous dissipation on unsteady MHD free convection flow past an infinite vertical plate in porous medium with time-dependent suction, *Int. Journal of Heat Mass Transfer*, (46) 13, 2305-2311, 2003.
- [5.] Lesnic, D.; Ingham, D. B.; Pop, I. and Storr, C.: Free convection boundary layer flow above a nearly horizontal surface in porous medium with Newtonian heating, *Heat and Mass Transfer*, (40)4, 665-672, 2003.
- [6.] Mazumdar M. K..and Deka R. K.: MHD flow past an impulsively started infinite vertical plate in presence of thermal radiation, *Romanian Journal of Physics*, (52)5:565 - 573, 2007.
- [7.] Merkin, J. H.: Natural convection boundary layer flow on a vertical surface with Newtonian heating, *International Journal Heat Fluid Flow*, (15) :392-398, 1994.
- [8.] Sangapatnam, S.; Nandanoor, B. R. and Vallampati, R. P.: Radiation and mass transfer effects on MHD free convection flow past an impulsively started isothermal vertical plate with dissipation, *Thermal Science*, (13):171-181, 2009.
- [9.] Stewarton, K.: On the impulsive Motion of a flat plate in a viscous fluid, *Quarterly Journal of Mechanics and Applied Mathematics*, (IV) 2, 182-198, 1951.
- [10.] Soundalgeka, V.M.: Free convection effects on the Stokes problem for infinite vertical plate, *ASME Journal of Heat Transfer*, 99, 499-501, 1977.
- [11.] Soundalgekar, V.M. Gupta, S. K. and Aranake, R. N. : Free convection effects on MHD Stokes problem for a vertical plate, *Nuclear Engg. Des.*, (51), 403-407, 1979.
- [12.] Takhar, H. S.; Gorla, R. S. R. and Soundalgekar, V. M.: Radiation effects on MHD free convection flow of a radiating fluid past a semi-infinite vertical plate, *Int. Journal of Numerical Methods for Heat and Fluid Flow*, (1), 77-83, 1996.
- [13.] Zucco Jordan, J.: Network simulation method applied to radiation and dissipation effects on MHD unsteady free convection over vertical porous plate, *Applied Math. Modelling*, (31) 20, 2019-2033, 2007.

Table 1. The skin friction τ for various values of F , M , G , Ec and Pr

	t=0.2	t=0.4	t=0.6	t=0.8
$Ec=0.1$	1.4538	0.93326	0.55158	0.2022
$Ec=0.3$	1.4003	0.84728	0.44199	0.074847
$Ec=0.6$	1.3211	0.72243	0.28553	-0.10485
$G=0$	1.7341	1.5227	1.4608	1.4363
$G=2$	1.4003	0.84728	0.44199	0.074847
$G=4$	1.0701	0.18708	-0.54816	-1.2532
$F=0$	1.3693	0.71044	0.10521	-0.579
$F=1$	1.4003	0.84728	0.44199	0.074847
$F=3$	1.4521	1.0387	0.83601	0.7152
$M=1$	1.166	0.52831	0.057828	-0.36901
$M=2$	1.4003	0.84728	0.44199	0.074847
$M=4$	1.8286	1.3912	1.0613	0.75701
$Pr=0.71$	1.2977	0.58413	-0.0314	-0.66033
$Pr=1.0$	1.4003	0.84728	0.44199	0.074847
$Pr=7.0$	1.6106	1.3215	1.2016	1.1319